Dissociative Electron Attachment to Anthralin to Model Its Biochemical Reactions

ARTICLE *in* JOURNAL OF PHYSICAL CHEMISTRY LETTERS · AUGUST 2014

Impact Factor: 7.46 · DOI: 10.1021/jz501523s

2 AUTHORS, INCLUDING:

Stanislav A Pshenichnyuk

Institute of Physics of Molecules and Crystals

58 PUBLICATIONS **294** CITATIONS

THE JOURNAL OF PHYSICAL CHEMISTRY Letters

Letter

pubs.acs.org/JPCL

Dissociative Electron Attachment to Anthralin to Model Its Biochemical Reactions

Stanislav A. Pshenichnyuk*[,†,‡] and Alexei S. Komolov[‡]

[†]Institute of Molecule and Crystal Physics, Ufa Research Centre, Russian Academy of Sciences, Prospekt Oktyabrya 151, 450075 Ufa, Russia

[‡]Physics Faculty, St. Petersburg State University, Uljanovskaja 1, 198504 St. Petersburg, Russia

ABSTRACT: The antipsoriatic drug anthralin (dithranol) is known to be extensively accumulated inside mitochondria of keratinocytes and to interact with the electron flow of the respiratory chain. Primary products of the one-electron reduction of polyphenolic anthralin observed in vivo are its dehydrogenated anions, which are formed by H-atom abstraction. The same species are mainly generated at low electron energies by dissociative electron attachment (DEA) to anthralin molecules in vacuo. A likely mechanism for the biochemical transformations of anthralin under reductive conditions in vivo is hypothesized on the basis of its DEA properties. The involvement of excited electronic states generated by ultraviolet irradiation of skin is discussed.

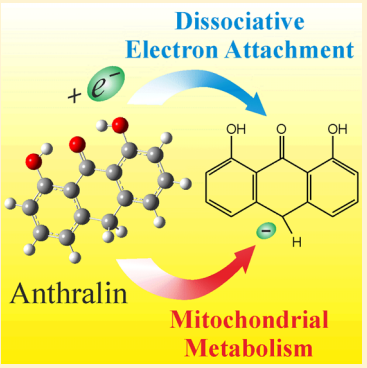

SECTION: Biophysical Chemistry and Biomolecules

Biological electron transfer is involved in many processes in the cells of living organisms and could be considered as the simplest biochemical reaction.[1] Electron transfer associated with the cleavage of covalent bonds, so-called dissociative electron transfer (DET),[2] is found to be an essential process in biochemistry and is driven by the capture of solvated electrons, by normally empty molecular orbitals (MOs), via resonance mechanisms.[3] In particular, the toxic effect in vivo of the model toxicant carbon tetrachloride (CCl_4) was first hypothesized by Gregory[4] to be associated with its gas-phase dissociative electron attachment (DEA) properties, which maintain essential features on going from the gas phase to the solution.[5] The one-electron reductive dehalogenation of CCl_4 by DET, a cellular process analogous to gas-phase DEA, was later discussed and postulated to be the main reason for the CCl_4 toxicity mediated by cytochrome P450 enzymes by generating trichloromethyl free radicals.[6,7] Christophorou and Hadjiantoniou suggested[8] that negative-ion resonances observed below 1 eV under gas-phase conditions could be involved in cellular electron transfer, owing to the stabilizing effect of the solvent on negative-ion states.

In addition to strongly bound (by 3.3 eV) solvated electrons localized in the bulk, electrons solvated at the interfaces are weakly bound by only 1.6 eV.[9] The formation of negative-ion states in water can efficiently proceed through the DEA mechanism by the transfer of surface-solvated electrons to a variety of organic molecules.[3] Recently, in a series of anti-inflammatory drugs, the involvement of DEA with cellular quasi-free electrons in the metabolic pathways of xenobiotic species was considered to be likely.[10] Additionally, mitochondrial dysfunction has been associated with unexpected species that are likely formed in cellular ambient by DEA in the well-known herbicides.[11]

Polyphenolic compounds, for instance, flavonoids, which are present in fruits and vegetables or spinochromes found in sea urchins, play essential roles in biochemical processes, revealing their antioxidant activity,[12] which can be associated with the DEA properties.[13] In particular, it has been shown that the elimination of two hydrogen atoms (located in the OH groups) from the negative ions of some flavonoids, formed by excess electron attachment, is accompanied by the formation of double C═O bonds. The reverse process, that is, reacquiring two H atoms to restore the initial phenolic structure, is only possible when the excess electron detaches.[13] This "recycling" is similar to a well-known process stimulated by the mitochondrial respiratory chain, and it consists of "switching" between the reduced ($CoQ_{10}H_2$) and oxidized (CoQ_{10}) forms of the cellular electron carrier ubiquinone (also known as Coenzyme Q_{10}). Although the oxidized form participates in cellular-energy biogenesis, the reduced form reveals antioxidant properties.[14]

The present study reports the gas-phase DEA properties of polyphenolic anthralin, which reveals biological activity against mitochondria and is extensively used clinically to treat psoriatic conditions.[15] In particular, its bioactivity is associated with its accumulation in mitochondria and interaction with the electron flow of the mitochondrial respiratory chain;[16,17] however, the exact molecular mechanism has not yet been elucidated.[18]

Received: July 20, 2014
Accepted: August 11, 2014
Published: August 11, 2014

Cellular oxygen is known to capture electrons that have "leaked" from the respiratory chain, which leads to the formation of superoxide anions and the generation of reactive oxygen species.[19] Provided that the electron affinity of anthralin is equal to (or higher than) that of O_2, it can compete for the quasi-free electrons and, in particular, can be fragmented via the DEA mechanism. The present data could, therefore, shed light on the molecular mechanisms of the biochemical reactions under reductive conditions. In particular, the data could be useful in the quickly growing field of mitochondrial medicine.[20,21]

Low-energy electron attachment to anthralin is investigated by DEA spectroscopy.[22,23] Our magnetic mass spectrometer has previously been described in detail.[24] In brief, a magnetically collimated electron beam of defined energy was passed through a collision cell containing a vapor of the substance under investigation, under single-collision conditions. A signal for the mass-selected negative ions was recorded as a function of the incident electron energy in the 0−14 eV energy range. The electron-energy scale was calibrated with the SF_6^- signal at zero energy, generated by the attachment of thermal electrons to SF_6. The full-width at half maximum (fwhm) of the electron-energy distribution was 0.4 eV, and the accuracy of the measured peak positions was estimated to be ±0.1 eV. The electron detachment time (τ_a) for mass-selected negative ions was measured as previously described.[25] The reference τ_a value for SF_6^- was estimated to be 120 μs at 100 °C. The substance under investigation (Sigma-Aldrich no. 10608) was evaporated at 90 °C, and the collision cell was held at 100 °C to prevent condensation.

To assign the experimental findings, density functional theory (DFT) calculations were performed with Gaussian 09 software.[26] The virtual orbital energies (VOEs) of the neutral molecules were evaluated using the B3LYP[27] hybrid functional with the standard 6-31G(d) basis set. Although the description of the anion states poses particular difficulties,[28] it has been demonstrated[29,30] that good linear correlations can be obtained between the experimental vertical attachment energies (VAEs) and the corresponding VOEs for the neutral molecules calculated with basis sets that do not include diffuse functions. Moreover, the scaling of VOEs was successfully used for the peak assignment of the experimentally obtained density of the unoccupied states in small conjugated molecular materials.[31,32] In the present study, the linear equation (VAE = 0.8065 × VOE + 0.9194) derived for the π^* MOs of alternating phenyl and ethynyl groups[33] was employed to scale the B3LYP/6-31G(d) π^* VOEs.

The first vertical electron affinity (EA_v) was also calculated as the difference between the total energy of the neutral state and the lowest anion state, both in the optimized geometry of the neutral state, using the standard 6-31+G(d) basis set with the minimum addition of diffuse functions. The adiabatic electron affinity (EA_a) was obtained as the energy difference between the neutral state and the lowest anion state, each in its optimized geometry. The thermodynamic energy thresholds for the formation of fragments by DEA were evaluated as the difference between their total energy and that of the neutral ground state. The effects of a solvated environment were evaluated using the polarizable continuum model (PCM).

According to the present B3LYP/6-31+G(d) calculations, the keto form of neutral anthralin (shown in Figure 1) is found to be the most stable in comparison with the OH rotational conformers and the enol structure; the conclusion, therefore, is

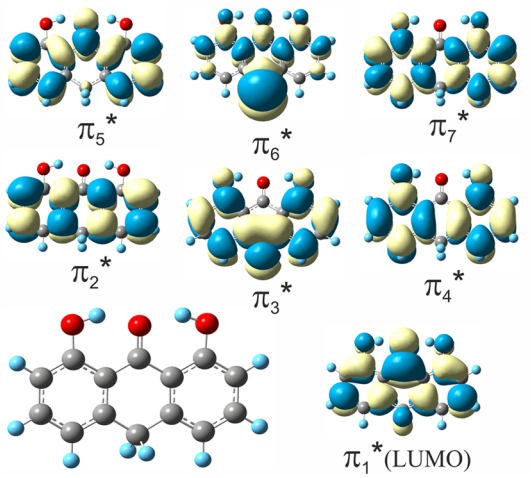

Figure 1. B3LYP/6-31+G(d) optimized geometry of the most stable neutral conformer of anthralin and representation of the localization properties of its π^* MOs, as supplied by B3LYP/6-31G(d) calculations.

in line with previously reported data.[34] Neutral anthralin molecules possess seven normally empty MOs of π type, which are schematically shown in Figure 1. The VOEs are listed in Table 1, along with the scaled VAE values. The VAEs predict

Table 1. B3LYP/6-31G(d) VOEs (eV) and Scaled Values (VAEs, See Text)

orbital	VOE	VAE
π_7^*	4.224	4.33
π_6^*	3.901	4.07
π_5^*	1.511	2.14
π_4^*	0.243	1.12
π_3^*	−0.255	0.71
π_2^*	−0.495	0.52
π_1^*	−2.116	−0.79

the energy positions of electron−molecule resonances.[22] Only the π_6^* orbital has a considerable contribution from the CH_2 group of the nonaromatic central ring, and the others mainly consist of combinations of benzene-like MOs from the anthracene core.

Currents of the mass-selected negative ions, formed by electron attachment to gas-phase anthralin, are presented in Figure 2a as a function of incident electron energy. The likely structures of the negative fragments, peak energies, and relative intensities are listed in Table 2. The most intense signal observed below 2 eV is due to the formation of long-lived negative ions at m/e = 226 (denoted as M^- in Table 2). The zero-energy peak is associated with electron addition to vibrationally excited levels of M^-, that is, the formation of vibrational Feshbach resonance.[22] Correspondingly, the π_1^* MO is predicted to lie in the bound region, with the first EA_v being evaluated at 0.79 eV. (See Table 1.) The shoulder at 0.7 eV in the m/e = 226 current is assigned to the unresolved contributions from the π_2^* and π_3^* shape resonances,[22] which are predicted at 0.52 and 0.71 eV, respectively. (See Table 1.)

An expanded view of the M^- current in comparison with that of SF_6^- (possessing instrumental shape) is reported in Figure 2b. Detection of the neutral counterpart[25] (labeled M^0), formed by electron detachment, allows an estimation of the mean

dx.doi.org/10.1021/jz501523s | J. Phys. Chem. Lett. 2014, 5, 2916−2921

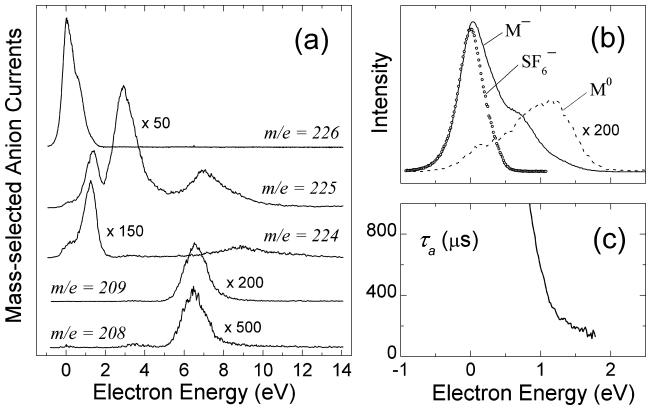

Figure 2. (a) Mass-selected signals of negative ions formed by DEA to gas-phase anthralin. (b) Yield of anthralin molecular negative ions (M^-, solid line) and of the corresponding neutral component (M^0, dashed line) and SF_6^- current (dots) as a function of incident electron energy. (c) Electron detachment time (τ_a) from M^- as a function of incident electron energy.

Table 2. Probable Structures of Fragment Negative Ions Observed in the DEA Spectra of Anthralin, Peak Energies (eV), and Relative Intensities Evaluated from the Peak Heights[a]

m/e	anion structure	peak energy	relative intensity
226	M^-	0.0	100
		0.7 sh.	
225	$[M - H]^-$	1.3	0.9
		2.9	1.9
		6.9	0.6
224	$[M - 2H]^-$	0.0 sh.	
		1.2	0.4
		9.0	0.1
209	$[M - OH]^-$	6.5	0.2
208	$[M - OH - H]^-$	3.5	<0.1
		6.5	0.1

[a]sh. stands for shoulder and M stands for anthralin.

electron-detachment time for M^-. The data presented in Figure 2c imply that anthralin molecular anions, formed by electron capture below 0.8 eV, maintain excess negative charge for >1 ms (which is outside of the present detection limit). In the range of 0.8 to 1.5 eV, τ_a decreases rapidly from 1 ms to 180 μs. Owing to faster electron detachment from the molecular anions formed with a high excess energy, the neutral counterpart in Figure 2b has a peak at 1.2 eV, likely due to electron detachment from the parent molecular anion formed through the π_4* resonance, predicted to lie at 1.12 eV by the scaled VOEs. (See Table 1.) The corresponding M^- signal in the DEA spectrum is plausibly masked by the more intense signal associated with the π_3* resonance.

In simple competition with extra electron detachment (τ_a = 280 μs at 1.2 eV), the negative molecular ions of anthralin, formed by electron addition to the π_4* MO, also decay via dissociation to produce dehydrogenated $[M-H]^-$ (m/e = 225) and doubly dehydrogenated $[M-2H]^-$ (m/e = 224) species close to 1.2 eV. (See Figure 2 and Table 2.) The more intense signal of the $[M-H]^-$ current is observed at 2.9 eV. This peak is almost equally distanced from the predicted positions of both the π_5* (2.14 eV) and π_6* (4.07 eV) resonant states and could be due to direct formation and decay of σ* resonance(s). In fact, it was suggested that DEA dehydrogenation of formic acid and glycine occurs through direct dissociation of a σ* (O−H) resonance and that it does not require π*/σ* coupling.[35] The calculations predict several σ* MOs in the energy range between the π_5* and π_6* MOs, but a scaling equation calibrated for σ* (O−H) or σ* (C−H) MOs is not available; thus, the data are not presented in Table 1. It is to be noted that the contribution from core-excited resonances[22] in this electron energy range cannot be ruled out. (B3LYP/6-31+G(d) energy for the lowest triplet $\pi-\pi$* transition in neutral anthralin is estimated to be 2.84 eV.) Elimination of a neutral hydroxyl group from the negative molecular ion to give the m/e = 209 negative fragment as well as loss of one additional H atom accounting for the m/e=208 signal is observed only at high energy (~6.5 eV). These peaks, as well as the one at 6.9 eV in the m/e = 225 current, lie above the π_7* MO (predicted at 4.33 eV) and are likely to be caused by core-excited resonances.[22]

The B3LYP6-31+G(d) thermodynamic-energy thresholds reported in Table 3 nicely account for the observed signals.

Table 3. B3LYP/6-31+G(d) Total Energies (eV) Relative to the Neutral Ground State of Anthralin in the Gas Phase and in Water[a]

		relative energy (eV)	
m/e	fragments	gas phase	water
226	vertical M^-	−1.04	−2.74
226	adiabatic M^-	−1.25	−2.94
225	$[M - H]^-$ + H· (from CH_2)	0.36	−1.29
225	$[M - H]^-$ + H· (from OH)	1.09	−0.94
225	$[M - H]^-$ + H· (from ring)	3.02	0.89
224	$[M - 2H]^-$ + H_2 (from OH and CH_2)	−0.67	−2.66
224	$[M - 2H]^-$ + H_2 (both from OH)	0.56	−1.47
224	$[M - 2H]^-$ + H_2 (from CH_2 and ring)	0.59	−1.04
224	$[M - 2H]^-$ + H_2 (both from CH_2)	0.62	−1.01
224	$[M - 2H]^-$ + H_2 (from OH and ring)	1.33	−0.70
209	$[M - OH]^-$	3.32	1.02
208	$[M - OH - H]^-$ + H_2O (H from CH_2)	0.60	−1.42
208	$[M - OH - H]^-$ + H_2O (H from OH)	1.44	−1.04
208	$[M - OH - H]^-$ + H_2O (H from ring)	2.41	0.12

[a]Values include zero-point vibrational energy corrections.

Hydrogen-atom elimination from the CH_2 group is expected to appear at 0.36 eV and is energetically more favorable than that from the OH group. Rupture of C−H bond in the aromatic ring requires 3.02 eV of energy and could account only for the peak at 6.9 eV in the m/e = 225 current. Abstraction of two H atoms from the molecular anion of gas-phase anthralin to form $[M-2H]^-$ is predicted to be exothermic, provided that both hydrogen atoms are eliminated from the CH_2 group, and a H_2 molecule is formed as a neutral counterpart. This finding accounts for the small signal observed at zero energy in the m/e = 224 current. According to the calculations (see Table 3), also the intense m/e = 224 peak observed at 1.2 eV must be accompanied by formation of H_2 molecules (calculated bond energy = 4.76 eV). Elimination of a neutral OH group is predicted to be possible at energies >3.32 eV and accounts for the m/e = 209 current. The B3LYP/6-31+G(d) dissociation energy of a H_2O molecule into OH and hydrogen is estimated to be 5.14 eV. Thus, the calculations indicate that the m/e = 208 negative fragment observed at 6.5 eV must be accompanied by the formation of a water molecule, with the only possible

dx.doi.org/10.1021/jz501523s | J. Phys. Chem. Lett. 2014, 5, 2916−2921

exception of abstraction of a H atom from the CH_2 group. (See Table 3.)

The estimated EA_a of anthralin is high enough to compete with cellular oxygen for electrons that are "leaked" into the mitochondrial intermembrane space from complex III,[36] as shown in Figure 3. The schematic view of the potential-energy

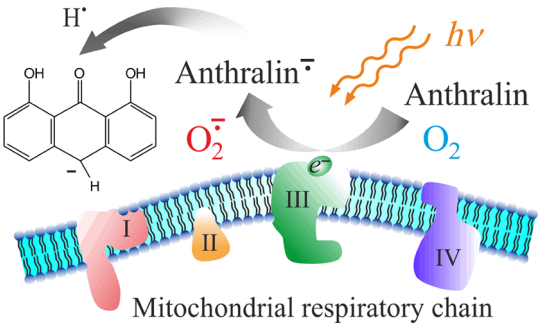

Figure 3. Likely analogy between electron attachment to cellular oxygen (EA_a = 0.45 eV) and exogenous anthralin (EA_a = 1.25 eV) in the mitochondrial intermembrane space. The former natural process leads to the production of reactive oxygen species, whereas the latter could produce a series of fragments by DEA. Possible UV irradiation of keratinocytes is indicated. Membrane complexes of the respiratory chain are labeled with roman numerals: I, NADH dehydrogenase; II, succinate dehydrogenase; III, cytochrome *bc*1 complex; IV, cytochrome *c* oxidase.

curves, for neutral anthralin and two anion states associated with extra electron addition into π_1* and π_4* MOs, are reported in Figure 4 in both gas-phase and aqueous environments. The Figure reflects a small stabilization (by 0.24 eV) of neutral anthralin (M) on going from the gas phase

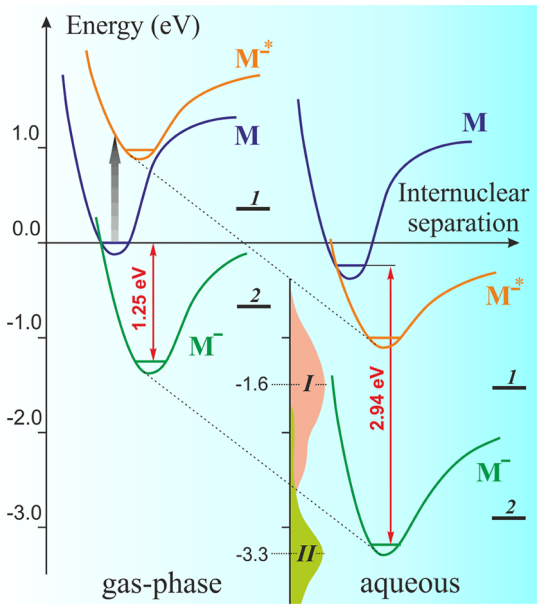

Figure 4. Potential energy curves for neutral anthralin (M), its ground-state anion (M^-), and the excited anion state (M^{-}*) associated with electron addition to the π_4* MO. Horizontal bars labeled ***1*** and ***2*** report asymptotic energies for formation of $[M - H]^- + H\cdot$ and $[M - 2H]^- + H_2$, respectively. The thick vertical arrow indicates attachment of a 1.12 eV electron to the π_4* MO. Energy distributions [3, 9] of partially hydrated and hydrated electrons in aqueous environment are labeled ***I*** and ***II***, respectively.

to a water solution. The positions of the anion ground states (M^-) in Figure 4 are derived from EA_a values (see Table 3) of isolated and aqueous anthralin (1.25 and 2.94 eV, respectively). The excited anion state (M^{-}*) in water is supposedly stabilized, similarly to the anion ground state, so that the distance between the M^- and M^{-}* terms is kept the same.

According to the semiquantitative picture, the anion ground state of aqueous anthralin could easily be accessible for bulk solvated electrons,[3,9] with binding energies corresponding to the high-energy wing of distribution ***II***. (See Figure 4.) Partially hydrated electrons (distribution ***I***) could occupy the vibrationally excited levels of M^- by a mechanism analogous to gas-phase vibrational Feshbach resonance,[22] and even the π_4* MO of solvated anthralin is accessible for the attachment of electrons from the high-energy wing of distribution ***I***, which is expected to produce the $[M-H]^-$ and $[M-2H]^-$ fragments. The present calculations imply that the final states of these fragments are strongly stabilized in water, such that the DEA process that is expected to be endothermic in vacuo becomes exothermic in the solvated state. (See Table 3 and Figure 4.) It leads to conclusion that the formation of $[M-H]^-$ and $[M-2H]^-$ could be possible near the mitochondrial respiratory chain by a cellular process analogous to gas-phase DEA. The energy barriers (or energies of intermediate states) for these transformations in cells are unknown. However, the tunneling process could be responsible for the elimination of light hydrogen atom(s) from the temporary negative ions. In fact, tunneling has been found to play an important role in intermolecular hydrogen transfer with phenolic compounds inside mitochondria.[37]

The direct formation of dehydrogenated free radicals of anthralin, owing to its reaction with peroxidizing lipids, has been observed in electron spin resonance studies.[38] The same $[M-H]^-$ species, associated with H atom abstraction from the CH_2 site in anthralin (structure is shown in Figure 3), are believed to be principal products of anthralin redox reactions[34] and have been considered as the main precursors of the bioactivity of anthralin, giving rise to the formation of reactive oxygen species, inhibiting respiration, and inducing apoptosis in keratinocytes.[15,39,40] According to the calculated thresholds (see Table 3), the CH_2 group is the preferred site for H atom elimination by DEA in anthralin. It is to be mentioned that the formation of two principal anthralin metabolites, danthron and an anthralin dimer,[39] must be initiated by H atom(s) abstraction from the CH_2 site, which could be attributed to DEA through a mechanism previously discussed in a series of anti-inflammatory drugs.[10]

UV excitation (3 to 4 eV) is known to reinforce the therapeutic action of anthralin.[41] It makes the generation of prehydrated electrons with binding energies close to zero possible through the excitation of bulk solvated electrons. The same conditions appear when natural sunlight irradiates psoriatic skin. As a result and according to considered Figure 4, the amount of electrons able to attain the π_4* MO of anthralin will increase, thus leading to the efficient generation of dehydrogenated radical species by DEA that, in turn, correlates with the increased biological activity. It is also to be mentioned that the anion state(s) responsible for the intense $[M-H]^-$ peak observed at 2.9 eV (see Figure 2 and Table 2) should be accessible for the presolvated electrons.

The role of the second likely product of DEA in cellular anthralin, that is, $[M-2H]^-$, is not obvious. Conversely to a series of flavonoids,[13] in which doubly dehydrogenated species

dx.doi.org/10.1021/jz501523s | J. Phys. Chem. Lett. 2014, 5, 2916−2921

are formed close to zero energy through H atom elimination of neighboring OH groups, the energetically preferred sites in anthralin are the OH and CH_2 groups. (See Table 3.) The formed anions are very long-lived (no neutral counterpart was detected) and probably serve as traps for electrons from the respiratory chain. The same activity could be ascribed to intact molecular anthralin anions, which are able to dissipate their energy to the surrounding media and thus escape dissociation or electron detachment. Because much anthralin is accumulated in mitochondria,[15] it could cause tight binding of the electrons of the respiratory chain, thus preventing respiration and inducing antipsoriatic and pro-inflammatory effects. Therefore, we hypothesize the important role of DEA to polyphenolic compounds, leading to the production of dehydrogenated species, as being a likely mechanism in biochemistry driven by biological electron transfer.

AUTHOR INFORMATION

Corresponding Author

*E-mail: sapsh@anrb.ru.

Notes

The authors declare no competing financial interest.

ACKNOWLEDGMENTS

We acknowledge Saint-Petersburg State University for research grants 11.38.219.2014 and 11.0.70.2010 and the Russian Foundation for Basic Research (grant #14-03-00087). We are also grateful to the reviewers for useful comments and suggestions.

REFERENCES

(1) Marcus, R. A.; Sutin, N. Electron Transfers in Chemistry and Biology. *Biochim. Biophys. Acta, Rev. Bioenerg.* **1985**, *811*, 265−322.

(2) Antonello, S.; Maran, F. Intramolecular Dissociative Electron Transfer. *Chem. Soc. Rev.* **2005**, *34*, 418−428.

(3) Abel, B.; Buck, U.; Sobolewski, A. L.; Domcke, W. On the Nature and Signatures of the Solvated Electron in Water. *Phys. Chem. Chem. Phys.* **2012**, *14*, 22−34.

(4) Gregory, N. L. Carbon Tetrachloride Toxicity and Electron Capture. *Nature* **1966**, *212*, 1460−1461.

(5) Wang, C. R.; Drew, K.; Luo, T.; Lu, M. J.; Lu, Q. B. Resonant Dissociative Electron Transfer of the Presolvated Electron to CCl4 in Liquid: Direct Observation and Lifetime of the CCl4*-Transition State. *J. Chem. Phys.* **2008**, *128*, 041102/1−4.

(6) Brattin, W. J.; Glende, E. A., Jr.; Recknagel, R. O. Pathological Mechanisms in Carbon Tetrachloride Hepatotoxicity. *Free Radical Biol. Med.* **1985**, *1*, 27−38.

(7) Manibusan, M. K.; Odin, M.; Eastmond, D. A. Postulated Carbon Tetrachloride Mode of Action: A Review. *J. Environ. Sci. Health, Part C* **2007**, *25*, 185−209.

(8) Christophorou, L. G.; Hadjiantoniou, D. Electron Attachment and Molecular Toxicity. *Chem. Phys. Lett.* **2006**, *419*, 405−410.

(9) Siefermann, K. R.; Liu, Y.; Lugovoy, E.; Link, O.; Faubel, M.; Buck, U.; Winter, B.; Abel, B. Binding Energies, Lifetimes and Implications of Bulk and Interface Solvated Electrons in Water. *Nat. Chem.* **2010**, *2*, 274−279.

(10) Pshenichnyuk, S. A.; Modelli, A. Electron Attachment to Antipyretics: Possible Implications of Their Metabolic Pathways. *J. Chem. Phys.* **2012**, *136*, 234307/1−11.

(11) Pshenichnyuk, S. A.; Modelli, A. Can Mitochondrial Dysfunction Be Initiated by Dissociative Electron Attachment to Xenobiotics? *Phys. Chem. Chem. Phys.* **2013**, *15*, 9125−9135.

(12) Nicholson, R. L.; Hammerschmidt, R. Phenolic Compounds and Their Role in Disease Resistance. *Annu. Rev. Phytopathol.* **1992**, *30*, 369−389.

(13) Modelli, A.; Pshenichnyuk, S. A. Gas-phase Dissociative Electron Attachment to Flavonoids and Possible Similarities to Their Metabolic Pathways. *Phys. Chem. Chem. Phys.* **2013**, *15*, 1588−1600.

(14) Frei, B.; Kim, M. C.; Ames, B. N. Ubiquinol-10 Is an Effective Lipid-Soluble Antioxidant at Physiological Concentrations. *Proc. Natl. Acad. Sci.* **1990**, *87*, 4879−4883.

(15) McGill, A.; Frank, A.; Emmett, N.; Turnbull, D. M.; Birch-Machin, M. A.; Reynolds, N. J. The Anti-Psoriatic Drug Anthralin Accumulates in Keratinocyte Mitochondria, Dissipates Mitochondrial Membrane Potential, and Induces Apoptosis Through a Pathway Dependent on Respiratory Competent Mitochondria. *FASEB J.* **2005**, *19*, 1012−1014.

(16) Salet, C.; Moreno, G.; Morliere, P.; Santus, R. Effects of Anthralin on Mitochondrial Bioenergetics. *Arch. Dermatol. Res.* **1991**, *283*, 186−190.

(17) Fuchs, J.; Zimmer, G.; Wölbling, R. H.; Milbradt, R. On the Interaction Between Anthralin and Mitochondria: A Revision. *Arch. Dermatol. Res.* **1986**, *279*, 59−65.

(18) Scatena, R.; Bottoni, P.; Botta, G.; Martorana, G. E.; Giardina, B. The Role of Mitochondria in Pharmacotoxicology: A Reevaluation of an Old, Newly Emerging Topic. *Am. J. Physiol.: Cell Physiol.* **2007**, *293*, C12−C21.

(19) Murphy, M. How Mitochondria Produce Reactive Oxygen Species. *Biochem. J.* **2009**, *417*, 1−13.

(20) Edeas, M.; Weissig, V. Targeting Mitochondria: Strategies, Innovations and Challenges: The Future of Medicine Will Come Through Mitochondria. *Mitochondrion* **2013**, *13*, 389−390.

(21) Koene, S.; Smeitink, J. Metabolic Manipulators: A Well Founded Strategy to Combat Mitochondrial Dysfunction. *J. Inherited Metab. Dis.* **2011**, *34*, 315−325.

(22) Schulz, G. J. Resonances in Electron Impact on Atoms. Resonances in Electron Impact on Diatomic Molecules. *Rev. Mod. Phys.* **1973**, *45*, 378−422, 423−486.

(23) Allan, M. Study of Triplet States and Short-Lived Negative Ions by Means of Electron Impact Spectroscopy. *J. Electron Spectrosc. Relat. Phenom.* **1989**, *48*, 219−351.

(24) Pshenichnyuk, S. A.; Asfandiarov, N. L. The Role of Free Electrons in MALDI: Electron Capture by Molecules of α-Cyano-4-hydroxycinnamic Acid. *Eur. J. Mass Spec.* **2004**, *10*, 477−486.

(25) Pshenichnyuk, S. A.; Vorob'ev, A. S.; Modelli, A. Resonance Electron Attachment and Long-lived Negative Ions of Phthalimide and Pyromellitic Diimide. *J. Chem. Phys.* **2011**, *135*, 184301/1−11.

(26) Frisch, M. J.; Trucks, G. W.; Schlegel, H. B.; Scuseria, G. E.; Robb, M. A.; Cheeseman, J. R.; Scalmani, G.; Barone, V.; Mennucci, B.; Petersson, G. A.; et al. *Gaussian 09*, revision A.02; Gaussian, Inc.: Wallingford, CT, 2009.

(27) Becke, A. D. Density-Functional Thermochemistry. III. The Role of Exact Exchange. *J. Chem. Phys.* **1993**, *98*, 5648−5652.

(28) Simons, J.; Jordan, K. D. Ab Initio Electronic Structure of Anions. *Chem. Rev.* **1987**, *87*, 535−555.

(29) Chen, D.; Gallup, G. A. The Relationship of the Virtual Orbitals of Self-Consistent-Field Theory to Temporary Negative Ions in Electron Scattering from Molecules. *J. Chem. Phys.* **1990**, *93*, 8893−8901.

(30) Modelli, A. Electron Attachment and Intramolecular Electron Transfer in Unsaturated Chloroderivatives. *Phys. Chem. Chem. Phys.* **2003**, *5*, 2923−2930.

(31) Pshenichnyuk, S. A.; Komolov, A. S. Relation between Electron Scattering Resonances of Isolated NTCDA Molecules and Maxima in the Density of Unoccupied States of Condensed NTCDA Layers. *J. Phys. Chem. A* **2011**, *116*, 761−766.

(32) Pshenichnyuk, S. A.; Kukhto, A. V.; Kukhto, I. N.; Komolov, A. S. Spectroscopic States of PTCDA Negative Ions and Their Relation to the Maxima of Unoccupied State Density in the Conduction Band. *Tech. Phys.* **2011**, *56*, 754−759.

(33) Scheer, A. M.; Burrow, P. D. π* Orbital System of Alternating Phenyl and Ethynyl Groups: Measurements and Calculations. *J. Phys. Chem. B* **2006**, *110*, 17751−17756.

(34) Czerwinska, M.; Sikora, A.; Szajerski, P.; Zielonka, J.; Adamus, J.; Marcinek, A.; Piech, K.; Bednarek, P.; Bally, T. Anthralin: Primary Products of Its Redox Reactions. *J. Org. Chem.* **2006**, *71*, 5312−5319.
(35) Gallup, G. A.; Burrow, P. D.; Fabrikant, I. I. Electron-Induced Bond Breaking at Low Energies in HCOOH and Glycine: The Role of Very Short-lived σ^* Anion States. *Phys. Rev. A* **2009**, *79*, 042701/1−7.
(36) Chen, Q.; Vazquez, E. J.; Moghaddas, S.; Hoppel, C. L.; Lesnefsky, E. J. Production of Reactive Oxygen Species by Mitochondria. Central Role of Complex III. *J. Biol. Chem.* **2003**, *278*, 36027−36031.
(37) Nagaoka, S. I.; Nishioku, Y.; Mukai, K. Tunneling Effect in the Regeneration Reaction of Vitamin E by Ubiquinol. *Chem. Phys. Lett.* **1998**, *287*, 70−74.
(38) Lambelet, P.; Ducret, F.; Löliger, J.; Maignan, J.; Reichert, U.; Shroot, B. The Relevance of Secondary Radicals in the Mode of Action of Anthralin. *Free Radical Biol. Med.* **1990**, *9*, 183−190.
(39) Müller, K. Antipsoriatic and Proinflammatory Action of Anthralin: Implications for the Role of Oxygen Radicals. *Biochem. Pharmacol.* **1997**, *53*, 1215−1221.
(40) Davies, A. G.; Hawari, J. A.; Whitefield, M. Generation and ESR Spectrum of the 1,8-Dihydroxy-9-Anthron-10-yl Radical. *Tetrahedron Lett.* **1983**, *24*, 4465−4468.
(41) Lapolla, W.; Yentzer, B. A.; Bagel, J.; Halvorson, C. R.; Feldman, S. R. A Review of Phototherapy Protocols for Psoriasis Treatment. *J. Am. Acad. Dermatol.* **2011**, *64*, 936−949.